

Article

# Analytical and Experimental Investigation of the Solar Chimney System

Zygmunt Lipnicki <sup>1,\*</sup>, Marta Gortych <sup>1</sup>, Anna Staszczuk <sup>1</sup>, Tadeusz Kuczyński <sup>1</sup> and Piotr Grabas <sup>2</sup>

<sup>1</sup> Faculty of Civil and Environmental Engineering, University of Zielona Góra, Z. Szafrana St. 1, 65-516 Zielona Góra, Poland; m.gortych@iis.uz.zgora.pl (M.G.); a.staszczuk@ib.uz.zgora.pl (A.S.); t.kuczynski@iis.uz.zgora.pl (T.K.)

<sup>2</sup> Department of Research and Innovation in Economy, University of Zielona Góra, Licealna St. 9, 65-417 Zielona Góra, Poland; piotrgrabas@poczta.fm

\* Correspondence: z.lipnicki@iis.uz.zgora.pl

Received: 29 March 2019; Accepted: 27 May 2019; Published: 29 May 2019



**Abstract:** In this paper the authors propose a new simplified method of solving the problem of air flow through a solar chimney system using a classical system of equations for the principles of conservation (momentum, mass, and energy), as well as a general solution to research the problem using similarity theory. The method presented in this paper allows one to design a solar chimney. The theoretical analysis was compared with experimental studies on existing solar towers. The experimental and theoretical studies were satisfactorily consistent. For clarity, the phenomenon of heat flow in the solar chimney was described using dimensionless numbers, such as the Reynolds, Grashof, Galileo, Biot, and Prandtl numbers. In the equations for the dimensionless geometric parameters, the ratios of the collector radius to the thickness gap, height, and chimney radius were used. The method used to test the system of equations allows us to analyse various solar collectors easily. In the scientific literature, there is a lack of a simple calculation method to use in engineering practice, suitable for each type of solar chimney independent of dimensions and construction parameters.

**Keywords:** solar chimney; air flow; analytical and experimental solutions; method of calculation

## 1. Introduction

Solar chimneys offer considerable potential for energy supply in countries abundant in sunlight. Especially in the last few decades this technology has been studied widely [1–4]. Researchers have focused on developing the technology of thermal solar energy, with potential applications worldwide. Kasaeian et al. [5] presented a comprehensive review of solar chimney systems. Depending on the research directions, solar chimneys may serve various goals [6–9], such as natural ventilation in the buildings [2,5,10–13], small-scale power plants, generation in full-scale energy generation systems, and some applications in smart islands [14–18].

A power plant consisting of a solar collector and a chimney can work as a solar thermal power plant [6,7,18–25], which first converts solar energy into thermal energy in the solar collector to further convert it into kinetic energy in the chimney, with final electricity generation by applying a wind turbine and generator [14,16,26]. The construction of such a solar chimney may depend on the shape and dimensions of both the collector and chimneys and their canopy profiles [10,27].

Most researchers focus on solving the problem of heat flow in solar chimneys using numerical simulations instead of analytical solutions. Compared to the analytical method, fewer assumptions are used in numerical simulations. However, it is possible to obtain more detailed descriptions of the temperature and flow field. The number of studies on numerical methods adopting computational

fluid dynamic programs (CFDs) to predict the efficiency of solar chimneys is constantly increasing. One of the first works using 2D numerical simulation to determine the temperature distribution and flow field in the collector was published by Pastohr et al. [28]. Similar numerical methods were used by Xu et al. [29,30]. Hamadan and Khashan [21] presented numerical results for a constant air flow inside the solar collector. The CFD analysis was used to determine the position of the turbine using the available power quantity. The CFD data showed that the height and size of the chimney are strongly related to each other, and the appropriate nozzle design at the entrance to the chimney is also important to reduce pressure losses. Koonsrisuk and Chitsomboon [31] developed a theoretical model that uses CFD analysis to conclude that the performance of a solar chimney with a sloping collector and divergent-top chimney is superior to a conventional chimney. In numerical 3D simulations, Guo et al. [32] validated experimental and numerical studies on the influence of solar radiation, turbine pressure drops, and ambient temperature on the solar collector's prototype in Manzanares, Spain. In the work of Abdelmohimen [33], the results of the collector tests from Manzanares were validated with the results of the numerical tests and proved to be consistent.

There are works discussing the problem of air flow through the solar collector system as an analytical issue. Pasumarthi and Sherif [34,35] developed an approximate model for studying the effect of various parameters on air temperature and velocity distribution in the system. Padki and Sherif [36] analyzed the solar collector system's efficiency, as influenced by the chimney, by developing an appropriate analytical model. This model allowed them to calculate the power output and efficiency of the solar chimney. Gannon and Von Backstrom [37] used a proposed mathematical model to apply a rotor for energy conversion in a solar chimney. They demonstrated that the use of blades to direct the air inlet resulted in improved system performance. Bernardes et al. [38] conducted a comprehensive analysis of analytical and numerical models describing the operation of a solar chimney power plant, which allowed them to estimate the output power of the solar chimneys. In addition, the influence of various environmental conditions and geometric dimensions on the power of solar chimneys was examined. The mathematical model has been used to predict the commercial performance of commercial solar chimneys on a large scale. It turned out that the height of the chimney, the pressure drop in the turbine, and the diameter of the chimney are of great importance [38]. Schlaich et al. [4] developed a mathematical model that is based on equations of momentum and energy conservation in solar chimney power plant. Zhou et al. [39] used a theoretical model to calculate the optimal chimney height for maximum output power. Guo et al. [40], in their model, considered the hourly changeability of solar radiation. It was shown that the output power increases almost linearly with the radius of the collector when the collector is small, assuming the use of an identical chimney. As the radius of the collector increases, this trend becomes slower. This process means that there is a limitation to the maximum radius of the collector above which there is no further increase in the output power. In the proposed analytical model of the solar chimney, Hamdan [41] obtained perfect compatibility with other published experimental and theoretical works. The obtained results indicate that the diameter of the collector and the diameter and height of the chimney and turbine are critical parameters for the construction of a solar plant. Kasaein et al. [5] reviewed experimental and theoretical studies of various solar collectors. They solved the system of equations for conservation of mass, momentum, and energy with appropriate boundary conditions for turbulent flows based on many experimentally determined parameters for air flowing through a chimney plant. While previous works show that the flow conditions inside the solar chimney can be well described theoretically, there is still a shortage of simple computational methods to be used in engineering practice, appropriate for each type of system, regardless of the dimensions and construction parameters. Therefore, this paper proposes a simplified method for solving the problem of air flow through the solar chimney. Again, this is based on the equations covering the principles of conservation (momentum, mass, and energy), and also the general solution of the problem using the theory of similarity. By using the original transformations of the equations describing the air flow in the solar chimney, combined with several additional assumptions, a system of equations was obtained, which allowed one to solve the problem analytically. This article

is a continuation of the previous work [15]. Some of the theoretical considerations have been repeated and refined. The theoretical model has been strengthened by taking into account the local resistance of the air flow between the collector and the chimney. The work also included experimental research conducted on the collector–chimney model, and the results of theoretical and experimental research were compared. Experimental and theoretical studies have shown satisfactory consistency. For greater clarity, the phenomenon studied was described using dimensionless numbers, such as the numbers of Reynolds, Grashof, Galileo, Biot, and Prandtl. In the equations for dimensionless geometrical parameters of the solar chimney, the ratio of the radius of the collector to its height, as well as the height and radius of the chimney, were applied. Based on the original transformations and simplifying assumptions, a system of equations was obtained that solved the problem analytically. A universal procedure for solving a complex problem has been developed for use in engineering, for the design of a solar chimney. The proposed method allows for an easy analysis of various solar collectors.

## 2. Theoretical Model of the Solar Chimney System

Theoretical model of the solar chimney system is shown in Figure 1.

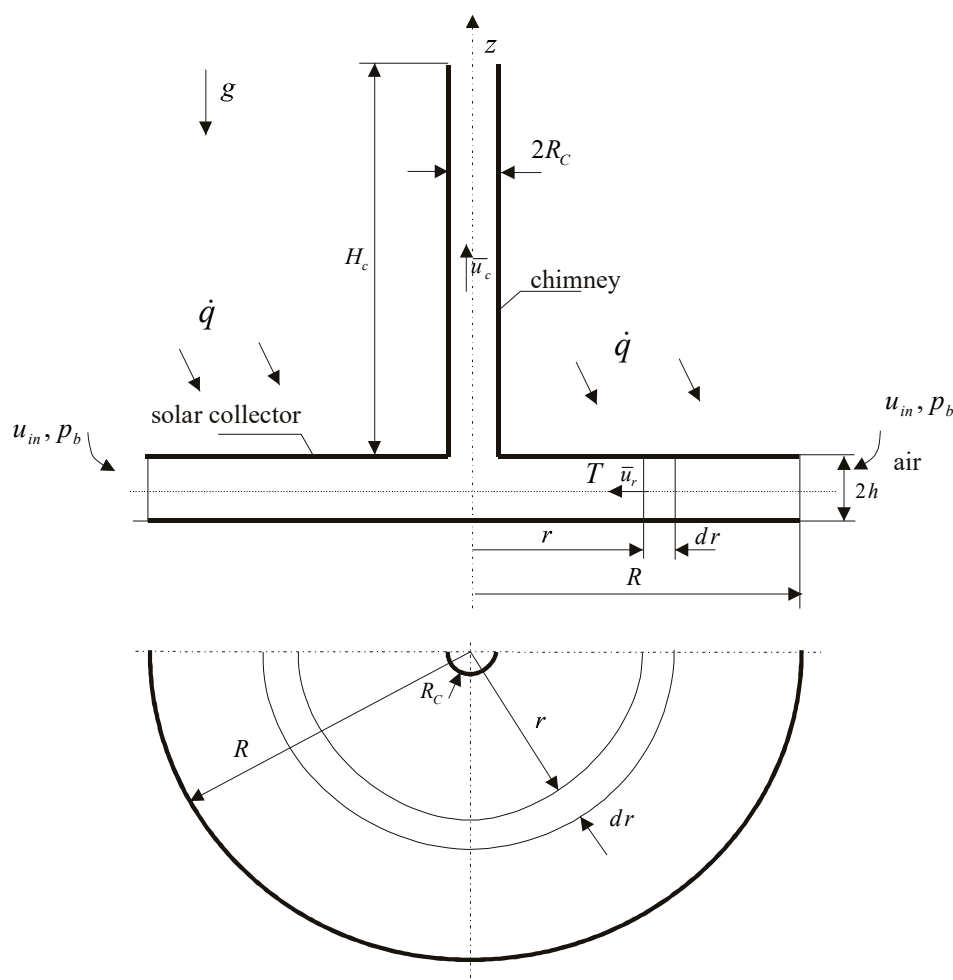


Figure 1. Solar chimney system.

The radius and height of the chimney are, respectively, represented by  $R_c$  and  $H_c$ . The distance between the top and bottom plates of the solar collector is constant and equal to  $2h$ , and the solar collector radius is represented by  $R$ . The absorbed solar radiation by the air flow in the collector is represented by  $\dot{q}$ . The velocity and pressure of the air flow at the entrance of the solar collector are,

respectively, represented by  $u_{in}$  and  $p_b$ , where the velocity of the air in the chimney is constant and equal to  $u_c$ . The distributed temperature of the air inside the collector is represented by  $T$ .

### 2.1. The Analysis of the Air Flow in the Solar Collector

The incompressible flow of air (with a constant viscosity) inside the collector (see Figure 1), the stationary Navier-Stokes equation and principle of the conservation of mass flux crossing cylindrical surfaces have the forms [15]:

$$-\frac{1}{\rho} \frac{\partial p}{\partial r} = u_r \frac{\partial u_r}{\partial r} - \nu \left[ \frac{1}{r} \frac{\partial}{\partial r} \left( r \frac{\partial u_r}{\partial r} \right) - \frac{u_r}{r^2} + \frac{\partial^2 u_r}{\partial z^2} \right] \text{ and } u_r r = \text{const}, \quad (1)$$

where equation  $u_r r = \text{const}$  results from the equation of conservation of mass.

After ignoring the small high-order parameters, the energy balance becomes

$$\dot{q} \cdot 2\pi \cdot r \cdot dr - 2\pi \cdot r \cdot dr \cdot \alpha(T - T_{ot}) = -2h \cdot \rho \cdot c_p \cdot 2\pi \cdot d(r \cdot \bar{u}_r \cdot T), \quad (2)$$

where  $\dot{q}$ ,  $\bar{u}_r$ ,  $T$ ,  $T_{ot}$ ,  $\rho$ ,  $\alpha$ ,  $c_p$ , and  $h$  represent the heat flux density and average radial velocity in the gap of the collector for the laminar flow, density of air, temperature of air, ambient temperature, and convective heat transfer coefficient between the ambient air and plate of the collector, the specific heat of air, and the depth of the collector, respectively.

By applying the boundary conditions at the collector inlet, we get

$$p = p_b, u = u_{in} \text{ and } T = T_{ot} \text{ for } r = R, \quad (3)$$

The solutions to Equations (1) and (2) (in dimensionless form) in the collector can be expressed as the dimensionless pressure drop and dimensionless distribution of temperature, respectively [15]:

$$\Pi = \frac{6}{5} \left( \frac{1}{\tilde{r}^2} - 1 \right) + \frac{6}{n\text{Re}} \ln \left( \frac{1}{\tilde{r}} \right); \theta = \tilde{q} \left\{ 1 - \exp \left[ -\frac{Bi\tilde{\lambda}}{4n\text{RePr}} (1 - \tilde{r}^2) \right] \right\}, \quad (4)$$

where the following dimensionless variables were introduced

$$\begin{aligned} \tilde{r} &= \frac{r}{R}; \Pi = \frac{2(p_b - p)}{\rho u_{in}^2}; \theta = \frac{T - T_{ot}}{T_{ot}}; \tilde{q} = \frac{\dot{q}}{\alpha T_{ot}}; \\ Bi &= \frac{\alpha h}{\lambda_s}; \tilde{\lambda} = \frac{\lambda_s}{\lambda}; \text{Re} = \frac{u_{in} h}{\nu}; \text{Pr} = \frac{\nu}{a}; n = \frac{h}{R}. \end{aligned}$$

Equation (4) was obtained from the solution of Equations (1) and (2) for laminar flow between the collector plates.

$$\theta(\tilde{q} = 3, Bi = 0.005, \text{Pr} = 0.712, \tilde{\lambda} = 2200, \text{ for } n = 0.04.)$$

As seen from the theoretical analysis (see Figure 2), the pressure drop and air temperature depend on the radial coordinates of the collector. As the Reynolds number increases, the air temperature in the collector increases more slowly. However, the influence of the Reynolds number on the pressure drop in the collector is negligible.

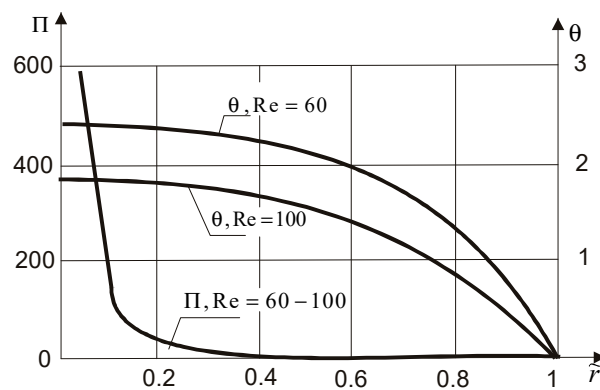


Figure 2. Distribution of dimensionless pressure drop,  $\Pi$ , and dimensionless temperature.

2.2. The Analysis of the Air Flow in the Solar Collector

For the chimney, the momentum equation of the flow of air inside the chimney (see Figure 1) in the cylindrical coordinate system  $(r, z)$ , with a vertical axis  $(z)$  directed upwards, can be written in the form

$$0 = -\frac{1}{\rho_c} \frac{\partial p_c}{\partial z} - g + \nu \left[ \frac{1}{r} \frac{\partial}{\partial r} \left( r \frac{\partial u_c}{\partial r} \right) \right]. \tag{5}$$

In Equation (5), we neglect the free convection in the solar collector. The density in the chimney describes the equation, and  $\rho_c = \rho[1 - \beta(T_c - T_{ot})]$  represents the density of air in the chimney, which depends on the increase in temperature  $(T_c - T_{ot})$ . We assume linear dependence of density on temperature. The temperature  $T_c$  in the chimney is constant, the coefficient of the thermal expansion of air is represented by  $\beta$ ,  $g$  represents the gravitational acceleration, and  $\nu$  represents the kinematic viscosity of air.  $p_c$  and  $u_c$  represent the pressure and velocity inside the chimney, respectively.

We apply the boundary conditions

$$\text{for } z = 0, p_c = \hat{p}_{CO} \text{ and } z = H_c, p_c = p_H, \tag{6}$$

where the following correlations are used in the above equations:

$$\hat{p}_{CO} = p_{CO} - \Delta p, p_H = p_b - \rho g H_c, \tag{7}$$

In the theoretical model, the local pressure ( $\Delta p$ ) in the flowing air between the solar collector and chimney is expressed as

$$\Delta p = \xi \frac{\rho_c \bar{u}_c^2}{2}, \tag{8}$$

where  $\xi$  represents the factor for the local loss in pressure in the air flow from the collector to the chimney, which results from the change of air flow direction and change of the channel cross-section between collector and chimney.

The velocity and average velocity in the chimney from the solution to the momentum equation (Equation (5)) are equal to

$$\begin{aligned} \tilde{u}_c &= \frac{1}{4\text{Re} \left( 1 - \theta \frac{Gr}{Ga} \right)} \left[ nGr\theta_c - \frac{1}{2} \widehat{\Pi}_{co} \frac{\text{Re}^2}{nm} \right] (\tilde{r}_c^2 - \tilde{r}^2), \\ \bar{\tilde{u}}_c &= \frac{1}{8\text{Re} \left( 1 - \theta_c \frac{Gr}{Ga} \right)} \left[ nGr\theta_c - \frac{1}{2} \widehat{\Pi}_{co} \frac{\text{Re}^2}{nm} \right] \tilde{r}_c^2. \end{aligned} \tag{9}$$

The dimensionless pressure drop,  $\widehat{\Pi}_{CO}$ , at the beginning of the chimney is equal to

$$\widehat{\Pi}_{CO} = \Pi_{CO} + \xi \frac{16n^2}{\left(1 - \frac{Gr}{Ga} \theta_c\right) \widetilde{r}_c^4},$$

where  $\Pi_{CO}$  represents the pressure drop calculated in the collector for  $\widetilde{r} = \widetilde{r}_c$ .

The velocity in the chimney, pressure drop at the beginning of the chimney, Reynolds number, Galileo number, Grashof number, and geometric parameter for the solar chimney can be presented in their dimensionless forms, respectively, as:

$$\widetilde{u}_c = \frac{u_c}{u_{in}}; \Pi_{CO} = \frac{2(p_b - p_{CO})}{\rho u_{in}^2}; \text{Re} = \frac{u_{in} h}{\nu}; Ga = \frac{g R^3}{\nu^2}, Gr = \frac{g \beta T_{ot} R^3}{\nu^2}; m = \frac{H_c}{R}.$$

The condition for the air flow in the chimney is calculated with Equation (9):

$$Gr \theta_c > \frac{\widehat{\Pi}_{CO} \text{Re}^2}{2n^2 m}. \quad (10)$$

From Equations (4) and (9), we achieve the coupled system below in Equation (11).

$$\begin{aligned} \frac{32n}{\widetilde{r}_c^4} &= \frac{nGr\theta_c - \frac{1}{2}\widehat{\Pi}_{CO}\frac{\text{Re}^2}{nm}}{\text{Re}}; \theta_c = \widetilde{q} \left\{ 1 - \exp\left[-\frac{Bi\widetilde{\lambda}}{4n\text{RePr}}(1 - \widetilde{r}_c^2)\right] \right\}; \\ \widehat{\Pi}_{CO} &= \Pi_{CO} + \xi \frac{16n^2}{\left(1 - \theta_c \frac{Gr}{Ga}\right) \widetilde{r}_c^4}; \Pi_{CO} = \frac{6}{5} \left( \frac{1}{\widetilde{r}_c^2} - 1 \right) + \frac{6}{n\text{Re}} \ln \frac{1}{\widetilde{r}_c}. \end{aligned} \quad (11)$$

Using the functions in the coupled system (Equation (11)),  $\theta_c(\text{Re})$ , and  $\widehat{\Pi}_{CO}(\text{Re})$  enable us to calculate the Reynolds number (Re) from the following equation:

$$f(\text{Re}) = \frac{nGr\theta_c - \frac{1}{2}\widehat{\Pi}_{CO}\frac{\text{Re}^2}{nm}}{\text{Re}} - \frac{32n}{\widetilde{r}_c^4} = 0. \quad (12)$$

The Reynolds number (Re) obtained from Equation (12) makes it possible to calculate the pressure drop  $\widehat{\Pi}_{CO}$  at the beginning of the chimney and the dimensionless temperature parameter  $\theta_c$  in the chimney.

$$T_o = 26 \text{ }^\circ\text{C}, h = 0.04 \text{ m}, R = 1 \text{ m}, R_c = 0.05 \text{ m}, \dot{q} = 800 \text{ W/m}^2, \alpha = 10 \text{ W/(m}^2\text{K)}.$$

For example, in Figure 3, the calculation of the Reynolds number was performed for the sample solar chimney system. Subsequently, the dimensionless parameters,  $\Pi_{CO}$  and  $\theta_c$ , were calculated.

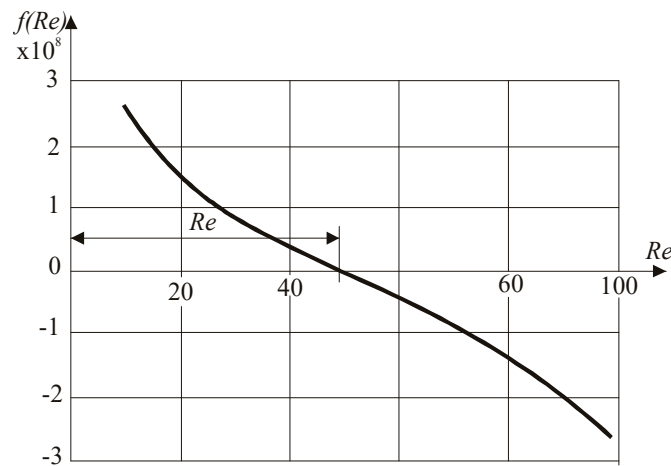


Figure 3. Example of the dependence of the function  $f(Re)$  on the Reynolds number ( $Re$ ) for.

Table 1 and Figure 4 display the air velocity  $\bar{u}_c$  and the air temperature  $T_c$  in the chimney.

Table 1. The air parameters in the chimney for  $T_o = 26\text{ }^\circ\text{C}$ ,  $h = 0.1\text{ m}$ ,  $R = 10\text{ m}$ ,  $R_c = 0.2\text{ m}$ ,  $\dot{q} = 800\text{ W/m}^2$ ,  $\alpha = 10\text{ W/(m}^2\text{K)}$ .

$H_c, \text{ m}$	$p_b - p_{co}, \text{ Pa}$	$\bar{u}_c, \text{ m/s}$	$T_c, \text{ }^\circ\text{C}$
5	2.39	3.75	106
10	4.65	5.23	105
15	6.59	6.23	104
20	8.85	7.22	103
30	12.40	8.55	100
40	17.65	10.20	97
50	20.15	10.91	96
100	37.64	14.92	88

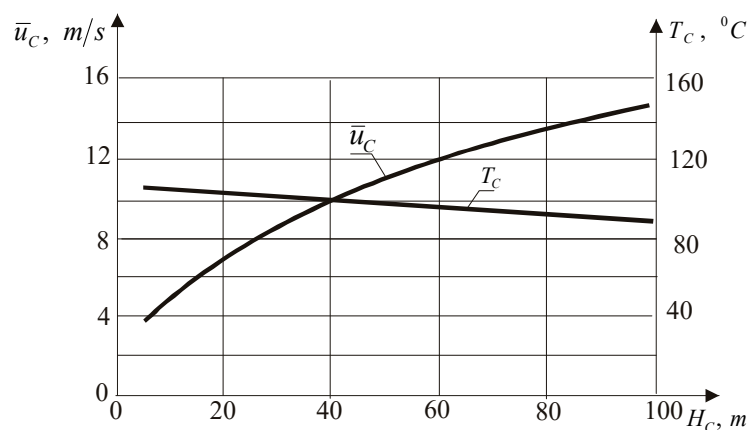
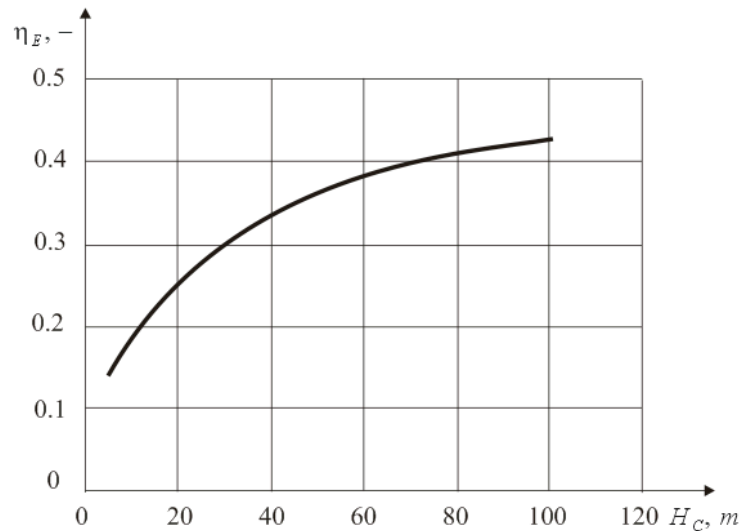


Figure 4. Dependence of air temperature ( $T_c$ ) and velocity ( $u_c$ ) on the height of the chimney ( $H_c$ ) for  $T_o = 26\text{ }^\circ\text{C}$ ,  $h = 0.1\text{ m}$ ,  $R = 10\text{ m}$ ,  $R_c = 0.2\text{ m}$ ,  $\dot{q} = 800\text{ W/m}^2$ ,  $\alpha = 10\text{ W/(m}^2\text{K)}$ .

The theoretical analysis on the turbulent flow of air is more challenging. In this case, the velocities of the air flows in the collector channel and chimney may be different. The theoretical model of air flow should be modified. Figure 4 presents the relationships of the height of the chimney with both the temperature (calculated according to Equation (4)) and velocity of the air inside the chimney (calculated according to Equation (9)). An increase in the chimney height causes an increase in air velocity and a decrease in air temperature. The increase in heat flux density increases both the temperature and air velocity in the chimney (see [15]).

Figure 5 shows the dependence of the energy efficiency of the solar chimney to the chimney height. Energy efficiency is the ratio of energy received to the energy supplied to the system. The energy obtained is the sum of the kinetic energy of the air and the increase in the enthalpy of the air. As shown in Figure 5, the energy efficiency of the solar chimney increases as the chimney height increases.



**Figure 5.** Energy efficiency  $\eta$  of the solar chimney as a function of chimney height, for  $\dot{q} = 800 \text{ W/m}^2$ ,  $R = 10 \text{ m}$ ,  $R_c = 0.2 \text{ m}$ .

Designing the solar chimney based on the proposed theoretical flow characteristics allows one to easily determine the energy efficiency of the chimney. Particularly noteworthy is the possibility of optimizing the chimney height with the goal of maximizing its efficiency, while maintaining construction costs at an acceptable level. In this way, the profitability of the installation plant can be significantly improved.

### 3. Experimental Investigation

Figure 6 shows the experimental model of the solar chimney, which consists of two low cylindrical collectors and a vertical, thermally insulated pipe placed in the middle of the plate.

The solar collector consists of two horizontal, flat disks forming an air gap spaced from each other. The diameter of the upper metal plate is 2000 mm, and the width of the air gap is 80 mm. In the middle of the board there is a vertical, thermally insulated pipe with an inner diameter of 100 mm and a height of 2500 mm.

Collector heating combined with the effect of a thermal chimney forces the airflow in the chimney. The velocity was measured using a paddle anemometer and Pitot tube. The Testo 417 anemometer was used for the measurements, which allows quick and precise measurements of air velocity from the chimney. The accuracy of the measurements was  $\pm 0.1 \text{ m/s}$ .

The results of the air velocity were measured with the paddle anemometer, which was mounted above the chimney. Then, the results of measurements were compared with the measurements using a Pitot tube, which was mounted on 2/3 of the chimney height, as shown in Figure 6. Moreover, the pressure drop at the collector's connection to the vertical pipe was measured using a differential inclined-tube manometer. The solar radiation flux was measured using a pyranometer located at a nearby meteorological station. The results of the measurements are presented in Table 2 and Figure 7.

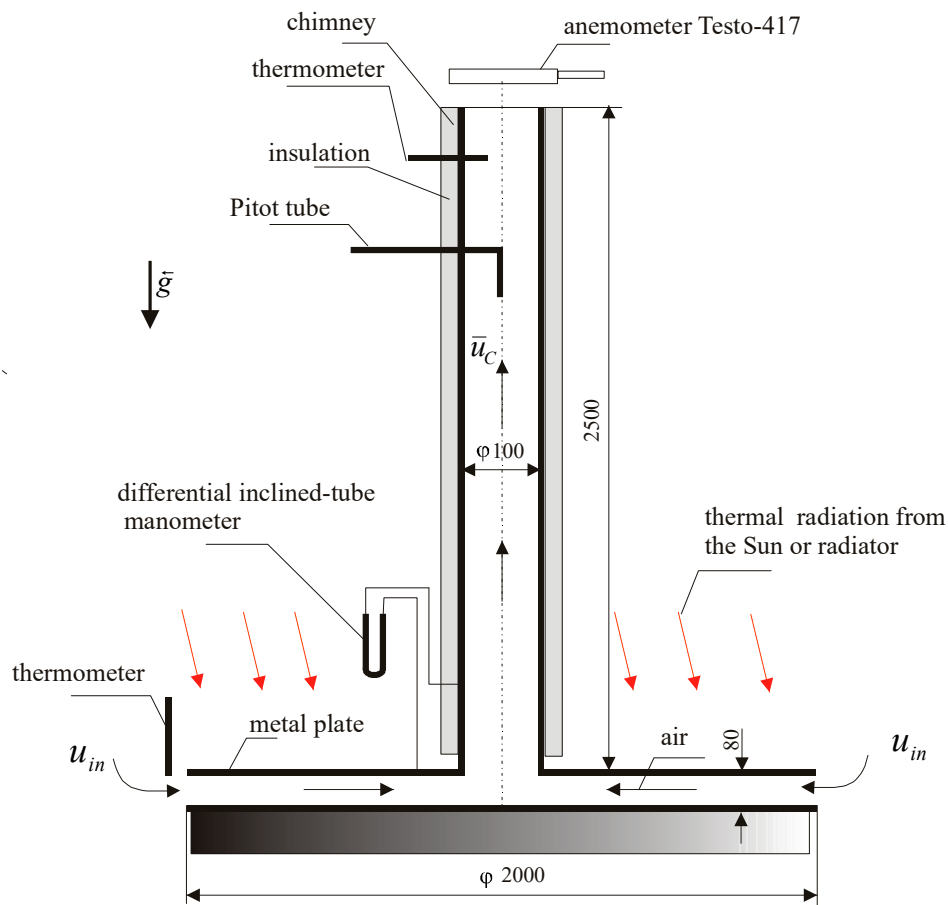


Figure 6. Experimental setup to validate the theoretical approach. Measured in mm.

Table 2. Results of experimental measurements.

No	1	22	3	4	5	6	7	8	9	10	11	12	13	14	15	16
$\dot{q}$ [ $W/m^2$ ]	145	150	400	550	600	610	680	710	715	730	790	800	800	840	845	920
$\dot{V}$ [ $m^3/h$ ]	19.8	21.2	19.8	25.2	17.2	17.0	22.3	21.2	20.9	20.9	28.3	28.3	31.1	28.3	25.4	19.8
$u_c$ [ $m/s$ ]	0.70	0.75	0.70	0.89	0.61	0.60	0.79	0.75	0.74	0.74	1.00	1.00	1.10	1.00	0.90	0.70

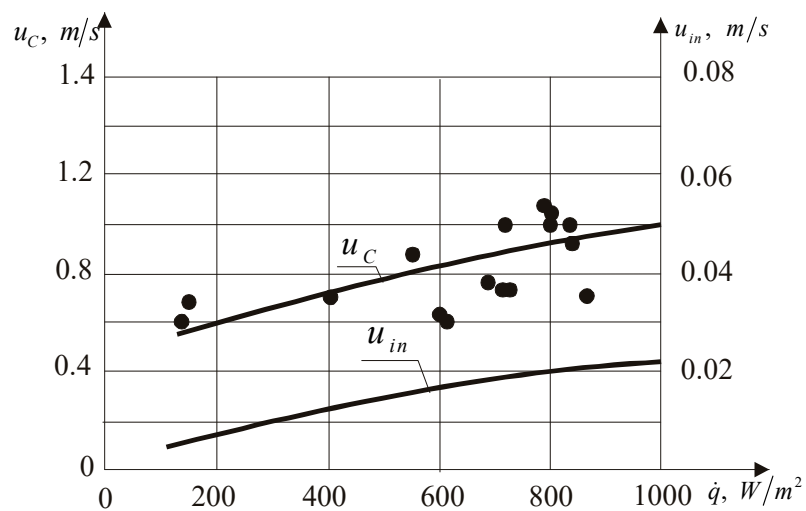


Figure 7. Comparison between the experimental and theoretical results.

Figure 7 presents a comparison of the results between theoretical studies (solid line) and experimental research (points) for the air velocity in the chimney, depending on the heat flux.

The results obtained in the analytical and experimental studies of the air velocity in the chimney are consistent and can be considered satisfactory. The scattering of results was mainly caused by disturbances caused by wind action between the collector plates on its perimeter. In this zone, the air flow velocities were very small (approximately  $0.02\text{ m/s}$ ), which was consistent with the theoretical model, and was, therefore, very sensitive to external gusts, which affected the operation of the solar chimney system.

#### 4. Conclusions

In this work, the obtained results of the experimental investigation and the theoretical considerations are satisfactory. The presented method is particularly suitable for laminar flow conditions in a collector (for relatively small systems, not for electricity generation). Under turbulent flow conditions (for larger systems with higher internal air velocities, which can be used for small-scale electricity generation), the results are less accurate, although their accuracy still seems to be acceptable at first. The approximated results are sufficient for the purpose of a design evaluation of solar collector–chimney systems. The considerations observe both the first and second principles of thermodynamics.

The paper presents the dependence of the energy efficiency of the solar collector system to the height of the chimney. It was shown that the energy efficiency of the solar collector system increases as the chimney height increases.

The presented modelling allows one to mimic very small systems, which is a foundation for future work to look into larger systems, up to the size of power plants.

**Author Contributions:** Conceptualization, Z.L., M.G., A.S., T.K. and P.G.; Methodology, Z.L., M.G., A.S., T.K. and P.G.; Validation, Z.L., M.G., A.S., T.K. and P.G.; Formal Analysis, Z.L., M.G., A.S., T.K.; Investigation, Z.L., P.G.; Writing—Original Draft Preparation, Z.L., M.G., A.S., T.K.; Writing—Review & Editing, Z.L., M.G., A.S., T.K.; Visualization, Z.L., M.G.; Supervision, Z.L., T.K.

**Funding:** This research received no external funding.

**Conflicts of Interest:** The authors declare no conflict of interest.

#### Nomenclature

$c_p$	specific heat at a constant air pressure, $\text{J kg}^{-1}\text{ K}^{-1}$ ;
$g$	gravitational acceleration, $\text{m s}^{-2}$ ;
$H_c$	chimney height, m;
$2h$	collector height, m;
$m$	ratio, $= H_c/R$ ;
$n$	ratio, $= h/R$ ;
$p$	pressure, Pa;
$p_b$	barometric pressure, Pa;
$p_{co}$	inlet pressure in the chimney, Pa;
$\dot{q}$	heat flux density, $\text{W m}^{-2}$ ;
$R$	radius of the collector, m;
$R_c$	radius of the chimney, m;
$T_{ot}$	ambient temperature, $^{\circ}\text{C}$ ;
$T$	temperature of air in the collector, $^{\circ}\text{C}$ ;
$T_c$	temperature of air in the chimney, $^{\circ}\text{C}$ ;
$u_c$	velocity in the chimney, $\text{m s}^{-1}$ ;
$u_{in}$	velocity input into the collector, $\text{m s}^{-1}$ ;
$z, r$	cylindrical coordinates, m;
$\alpha$	convective heat transfer coefficient, $\text{W m}^{-2}\text{K}^{-1}$ ;

$\lambda$	heat conductivity of air, $\text{W m}^{-1}\text{K}^{-1}$ ;
$\lambda_s$	heat conductivity of the plate collector, $\text{W m}^{-1}\text{K}^{-1}$ ;
$\xi$	local factor for pressure loss,
$\nu$	kinematic viscosity of air, $\text{m}^2\text{s}^{-1}$ ;
$\rho$	density of air, $\text{kg m}^{-3}$ ;
$\tilde{u}_c$	dimensionless velocity in the chimney;
$\tilde{r}_c$	dimensionless radius in the chimney;
$\tilde{r}$	dimensionless radius in the collector;
$\tilde{q}$	dimensionless heat flux density;
$\Pi$	dimensionless pressure;
$\theta$	dimensionless temperature;
$Bi$	Biot number;
$Ga$	Galileo number;
$Gr$	Grashof number;
$Pr$	Prandtl number;
$Re$	Reynolds number.

## References

- Haaf, W.; Friedrich, K.; Mayr, G.; Schlaich, J. Solar Chimneys—Part I: Principle and Construction of the Pilot Plant in Manzanares. *Int. J. Sol. Energy* **1983**, *2*, 3–20. [\[CrossRef\]](#)
- Maia, C.B.; Ferreira, A.G.; Valle, R.M.; Cortez, M.F.B. Theoretical evaluation of the influence of geometric parameter and materials on the behavior of the airflow in a solar chimney. *Comput. Fluids* **2009**, *38*, 625–636. [\[CrossRef\]](#)
- Schlaich, J. *The Solar Chimney. Electricity from the Sun*; Edition Axel Menges: Stuttgart, Germany, 1995.
- Schlaich, J.; Bergemann, R.; Schiel, W.; Weinrebe, G. Sustainable electricity generation with solar updraft towers. *Struct. Eng. Int.* **2003**, *3*, 222–229. [\[CrossRef\]](#)
- Kasaeian, A.B.; Molana, S.; Rahmani, K.; Wen, D. A review on solar chimney systems. *Renew. Sustain. Energy Rev.* **2017**, *67*, 954–987. [\[CrossRef\]](#)
- Chergui, T.; Larbi, S.; Bouhdjar, A. Thermo-hydrodynamic aspect analysis of flows in solar chimney power plants—a case study. *Renew. Sustain. Energy Rev.* **2010**, *14*, 1410–1418. [\[CrossRef\]](#)
- Maia, C.B.; Castro, J.O.; Cabezas-Gómez, L.; Hanriot, S.M.; Ferreira, A.G. Energy and exergy analysis of the airflow inside a solar chimney. *Renew. Sustain. Energy Rev.* **2013**, *27*, 350–361. [\[CrossRef\]](#)
- Naeeni, N.; Yaghoubi, M. Analysis of wind flow around a parabolic collector (1) fluid flow. *Renew. Energy* **2007**, *32*, 1898–1916. [\[CrossRef\]](#)
- Naeeni, N.; Yaghoubi, M. Analysis of wind flow around a parabolic collector (2) heat transfer from receiver. *Renew. Energy* **2007**, *32*, 1259–1272. [\[CrossRef\]](#)
- Bansal, N.K.; Mathur, J.; Mathur, S.; Jain, M. Modeling of window-sized solar chimneys for ventilation. *Build. Environ.* **2005**, *40*, 1302–1308. [\[CrossRef\]](#)
- Khanal, R.; Lei, C. A numerical investigation of buoyancy induced turbulent air flow in an inclined passive wall solar chimney for natural ventilation. *Energy Build.* **2015**, *93*, 217–226. [\[CrossRef\]](#)
- Khanal, R.; Lei, C. A scaling investigation of the laminar convective flow in a solar chimney for natural ventilation. *Int. J. Heat Fluid Flow* **2014**, *45*, 98–108. [\[CrossRef\]](#)
- Layeni, A.T.; Nwaokocha, C.N.; Giwa, S.O.; Olamide, O.O. Numerical and Analytical Modeling of Solar for Chimney Combined Ventilation and Power in Buildings. *Covenant J. Eng. Technol.* **2018**, *2*, 36–58.
- Li, J.; Guo, P.; Wang, Y. Effects of collector radius and chimney height on power output of a solar chimney power plant with turbines. *Renew. Energy* **2012**, *47*, 21–28. [\[CrossRef\]](#)
- Lipnicki, Z.; Gortych, M.; Staszczuk, A.; Kuczyński, T. The theoretical analysis of mass and energy flow through solar collector—Chimney system. *Civ. Environ. Eng. Rep.* **2017**, *24*, 117–131. [\[CrossRef\]](#)
- Mekhail, T.; Rekaby, A.; Fathy, M.; Bassily, M.; Harte, R. Experimental and Theoretical Performance of Mini Solar Chimney Power Plant. *J. Clean Energy Technol.* **2017**, *5*, 294–298. [\[CrossRef\]](#)
- Papageorgiou, C. Floating solar chimney with multi-pole generators. In Proceedings of the IASTED International Conference on Power and Energy System, Crete, Greece, 22–24 June 2011; pp. 60–65.

18. Cannistraro, G.; Cannistraro, M.; Trovato, G. Islands “Smart Energy” for Eco-Sustainable Energy a Case Study “Favignana Island”. *Int. J. Heat Technol.* **2017**, *35*, S87–S95. [[CrossRef](#)]
19. Asnaghi, A.; Ladjevardi, S.M. Solar chimney power plant performance in Iran. *Renew. Sustain. Energy Rev.* **2012**, *16*, 3383–3390. [[CrossRef](#)]
20. Azizian, K.; Yaghoubi, M.; Niknia, I.; Kanan, P. Analysis of Shiraz Solar Thermal Power Plant Response Time. *J. Clean Energy Technol.* **2013**, *1*, 22–26. [[CrossRef](#)]
21. Hadman, M.O.; Khashan, S. Numerical Investigation of Solar Chimney Power Plant in UAE. In *ICREGA'14—Renewable Energy: Generation and Applications*; Springer Proceedings in Energy; Springer: Cham, Switzerland, 2014; pp. 513–524.
22. Hamdan, M.O. Analytical Thermal Analysis of Solar Chimney Power Plant. In Proceedings of the ASME 2010 4th International Conference on Energy, Phoenix, AZ, USA, 17–22 May 2010.
23. Sangi, R. Performance evaluation of solar chimney power plants in Iran. *Renew. Sustain. Energy Rev.* **2012**, *16*, 704–710. [[CrossRef](#)]
24. Tayebi, T.; Djezzar, M. Numerical Analysis of Flows in a Solar Chimney Power Plant with a Curved Junction. *Int. J. Energy Sci.* **2013**, *3*, 280–286.
25. Zhou, X.; Wang, F.; Ochieng, R.M. A review of solar chimney power technology. *Renew. Sustain. Energy Rev.* **2010**, *14*, 2315–2338. [[CrossRef](#)]
26. Hanna, M.B.; Mekhail, T.A.M.; Dahab, O.M.; Esmail, M.F.C.; Abdel-Rahman, A.R. Experimental and Numerical Investigation of the Solar Chimney Power Plant’s Turbine. *Open J. Fluid Dyn.* **2016**, *6*, 332–342. [[CrossRef](#)]
27. Cottam, P.J.; Duffour, P.; Lindstrand, P.; Fromme, P. Effect of canopy profile on solar thermal chimney performance. *Sol. Energy* **2016**, *129*, 286–296. [[CrossRef](#)]
28. Pastohr, H.; Kornat, O.; Gurlebeck, K. Numerical and Analytical Calculations of the Temperature and Flow Field in the Upwind Power Plant. *Int. J. Energy Res.* **2004**, *28*, 495–510. [[CrossRef](#)]
29. Xu, G.L.; Ming, T.Z.; Pan, Y.; Meng, F.L.; Zhou, C. Numerical analysis on the performance of solar chimney power plant system. *Energy Convers. Manag.* **2011**, *52*, 876–883. [[CrossRef](#)]
30. Xu, H.; Karimi, F.; Yang, M. Numerical investigation of thermal characteristics in a solar chimney projects. *J. Sol. Energy Eng.* **2014**, *136*, 011008. [[CrossRef](#)]
31. Koonsrisuk, A.; Chitsomboon, T. Effects of flow are a changes on the potential of solar chimney power plants. *Energy* **2013**, *51*, 400–406. [[CrossRef](#)]
32. Guo, P.; Li, J.; Wang, Y. Numerical simulation of solar chimney power plant with radiation model. *Renew. Energy* **2014**, *62*, 24–30. [[CrossRef](#)]
33. Abdelmohimen, M.A.H.; Algarin, A.A. Numerical investigation of solar chimney power plants performance for Saudi Arabia weather conditions. *Sustain. Cities Soc.* **2018**, *38*, 1–8. [[CrossRef](#)]
34. Pasumarthi, N.; Sherif, S.A. Experimental and theoretical performance of a demonstration solar chimney model: Part I: Mathematical model development. *Int. J. Energy Res.* **1998**, *22*, 277–288. [[CrossRef](#)]
35. Pasumarthi, N.; Sherif, S.A. Experimental and theoretical performance of a demonstration solar chimney model: Part II: Experimental and theoretical results and economic analysis. *Int. J. Energy Res.* **1998**, *22*, 443–461. [[CrossRef](#)]
36. Padki, M.; Sherif, S. On a simple analytical model for solar chimneys. *Int. J. Energy Res.* **1999**, *23*, 345–349. [[CrossRef](#)]
37. Gannon, A.J.; Von Backström, T.W. Controlling and maximizing solar chimney power output. In Proceedings of the 1st International Conference on Heat Transfer, Fluid Mechanics and Thermodynamics, Kruger Park, South Africa, 8–10 April 2002.
38. Bernardes, M.A.; Weinrebe, A.V.G. Thermal and technical analyses of solar chimneys. *Sol. Energy* **2003**, *75*, 511–524. [[CrossRef](#)]
39. Zhou, X.; Yang, J.; Xiao, B.; Hou, G. Analysis of chimney height for solar chimney power plant. *Appl. Therm. Eng.* **2009**, *29*, 178–185. [[CrossRef](#)]

40. Guo, P.; Li, J.; Wang, Y. Annual performance analysis of the solar chimney power plant in Sinkiang, China. *Energy Convers. Manag.* **2014**, *87*, 392–399. [[CrossRef](#)]
41. Hamdan, M.O. Analysis of solar chimney power plant utilizing chimney discrete model. *Renew. Energy* **2013**, *56*, 50–54. [[CrossRef](#)]



© 2019 by the authors. Licensee MDPI, Basel, Switzerland. This article is an open access article distributed under the terms and conditions of the Creative Commons Attribution (CC BY) license (<http://creativecommons.org/licenses/by/4.0/>).